Triple-point wetting of molecular hydrogen isotopes

Masoud Sohaili[1], Jürgen Klier and Paul Leiderer

Department of Physics, University of Konstanz, D-78457 Konstanz, Germany

E-mail: masoud.sohaili@uni-konstanz.de

Abstract
Triple-point wetting is a well-known phenomenon of simple adsorbates on
solid substrates, which involves, in the liquid phase above the triple-point
temperature, T_3, complete wetting with the formation of arbitrary thick films
being observed, whereas below T_3 only a few monolayers of the solid phase
are adsorbed at saturated vapour pressure. This effect is usually ascribed
to the substrate-induced strain in the solid film, which occurs due to the
lattice mismatch and the strong van der Waals pressure in the first few
monolayers. Molecular hydrogen is a suitable system in which to investigate
this phenomenon, in particular by tailoring the adsorbate–substrate interaction
by means of thin preplating layers of other adsorbates, and by introducing
disorder into the system by using not only the pure systems H_2 and D_2, but also
mixtures thereof. The experiments show that triple-point wetting is a rather
dominant effect which, in contrast to expectations, persists even if the system
parameters are widely varied. This indicates that the present understanding of
this effect is incomplete. We present an investigation of the influence of the
roughness of the substrate which is expected to be responsible for the dewetting
of the solid phase.

1. Introduction

Wetting and dewetting of physisorbed films have been studied extensively both theoretically
[1–5] and experimentally [8–25]. A number of reviews on this subject, like those by Dietrich [6]
and Schick [7], exist. There are two ways in which multilayer films can grow on an attractive
substrate. In the first, the thickness of the film increases with increasing pressure, and diverges
as the vapour pressure approaches the saturated value (complete wetting). In the second, the
thickness of the film remains finite at bulk coexistence (incomplete–partial wetting). For a
given adsorbate and substrate combination a transition may occur from incomplete to complete
wetting as a function of temperature [2].

[1] Author to whom any correspondence should be addressed.

Triple-point wetting is described as a transition from an incomplete wetting solid film to a complete wetting liquid film at its triple point, T_3 [14]. In the early theories lattice mismatch between the film and the substrate was considered to be responsible for the finite thickness of the solid film [4, 5].

The majority of measurements have been devoted to adsorption isotherms of rare gases on graphite [8–10], Ag [11], MgO [12], CO_2 [13], and Au [14, 15], which were mostly in the thickness range of one to ten monolayers. Multilayer H_2 films have been studied on graphite substrates via volumetric adsorption isotherms [16] and ellipsometry [17] or on Ag via a quartz crystal microbalance [18]. Intensive investigations of H_2 on Au and preplated Au substrates have been the subject of a series of experiments [19–21] in which the surface plasmon spectroscopy technique was used. Films of H_2–D_2 mixtures [22, 23] and thick quench-condensed films [24–27] have been investigated via these methods. A few measurements [28, 29] have also been performed on the surface of Si. There are hints that strain in the solid films, induced by surface roughness, is important for T_3 dewetting, in addition to the lattice mismatch effects mentioned above.

Thick solid films of H_2 isotopes have subtle fundamental applications and it is therefore also important from this practical point of view to understand the incomplete wetting of these films below T_3. Solid H_2 films can be used as a substrate [30–32] to hold electrons at a distance above them. Preparation of thick solid T_2 films plays a decisive role in experiments designed to measure the neutrino rest mass [33–35] and solid D_2 films in nuclear fusion [36, 37]. Moreover, H_2 films, which due to their light molecular mass have a quantum nature, offer another system for studying relationships which may exist between the quantum nature of a system and its wetting properties. For example, H_2 superfluidity on relatively thick solid layers of H_2 has been predicted [38, 39].

The outline of this paper is as follows. In section 2 we briefly give some theoretical background and recent advances which are related to this work. The experimental methods used for the measurements are explained in section 3. Achievements and results are presented and discussed in section 4.

2. Theoretical background

In contrast to chemisorption, where chemical bounds are formed upon adsorption, physisorption involves formation of one or more layers of an adsorbate on a surface attracted by the substrate potential. Since typical potential depths range from a few kelvins to a few 100 K [40], depending on the system, physisorption can be initiated by sufficiently lowering the temperature such that the thermal excitations become small compared to the potential depth of the substrate. In general, the interaction potential between two atoms or molecules at a distance from each other is described by the Lennard-Jones (LJ) potential [41].

In the case of an atom (or molecule) a distance z away from a surface the proper interaction potential, $\phi(z)$, can be obtained by summing over all pairwise LJ-based interactions of the single adsorbate with the substrate atoms filling the half-space. The calculation [42] gives

$$\phi(z) = \frac{4C_3^3}{27D^2z^9} - \frac{C_3}{z^3}, \tag{1}$$

where C_3 and D are the van der Waals (vdW) coefficient and the potential depth, respectively. At large distances the attractive part of this potential becomes dominant. This term has a z^{-3} dependence, and so a weak long range interaction. This potential explains the wetting of liquid adsorbates on solid substrates correctly.

When studying the wetting of *solid* adsorbates on solid substrates the effect of the substrate on wetting becomes more crucial, since in this case the structural mismatch between the
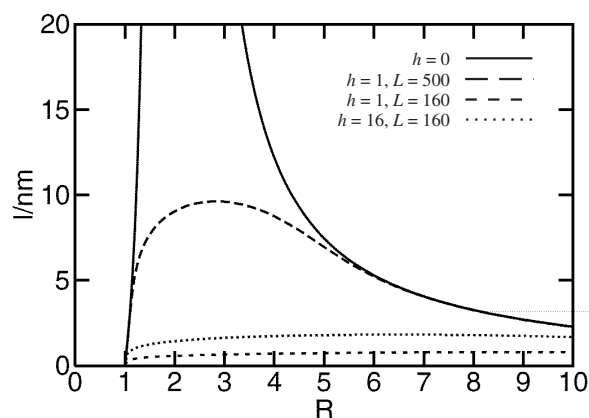
Figure 1. Comparison between the result of the former theory [5] and those of [43], for four different scales of roughness. The thickness of the solid film, l, increases as roughness vanishes. The parameters h and L are typical scales for the substrate roughness as explained in figure 2; R is the relative substrate strength.

substrate and the adsorbate causes so-called *strain-induced* forces in the adsorbed film. In this respect, the theory given by Gittes and Schick (GS) [5] has initially addressed the case of solid noble gases on graphite. This has recently been elaborated on and adapted for other practical substrates by Esztermann *et al* [43]. Since these theories are of crucial importance to the measurements reported in this paper, we briefly point out their principles and predictions. The equilibrium thickness is calculated by minimizing the total excess free energy $\Sigma(l_s, l_l)$ with respect to l_s and l_l, the solid and liquid thicknesses of the adsorbate, respectively. By definition, $\Sigma = \Omega/A$, where Ω is the excess grand canonical free energy relative to a non-wetting situation and A is the surface area.

The total excess free energy may be split into three different terms:

$$\Sigma_{\text{total}} = \Sigma_{\text{thrm}} + \Sigma_{\text{GS}} + \Sigma_{\text{EL}}, \tag{2}$$

where Σ_{thrm} results from thermodynamics. Σ_{GS}, calculated by GS, is caused by the lateral induced strain in the solid adsorbate. Σ_{EL}, considered as an additional term by [43], accounts for the free energy cost, caused by substrate roughness.

In figure 1, the results from both theories are shown. Plotted is the equilibrium thickness of the adsorbate versus the relative substrate strength R. The solid curves are the result of GS, i.e., the first two terms in equation (2). The dashed curves are the results from [43], taking a finite substrate roughness into account.

The experimental results display serious deviations from the prediction of GS. For example, as will be shown in section 4, a solid H_2 film always dewets a gold substrate below its T_3, and the thickness of the H_2 film becomes of the order of a few molecular layers. According to the GS theory a considerable film thickness of around 100 Å (essentially complete wetting) should be achievable for H_2 on Au (at $R \approx 4.5$); see figure 1. One possible reason for the discrepancy could be that the GS theory ignores substrate roughness which is a general property of real surfaces. This, as a result, causes an additional bending of the adsorbed solid film, considered by the new theory in [43]. Depending on the finite roughness of the substrate, the wetting of a solid adsorbate is suppressed, and the solid adsorbed film becomes thinner as the roughness scale increases. For typical substrates, the surface modulation varies on a characteristic lateral length scale L which is much larger than the vertical valley to peak distance h, i.e., $L \gg h$ (see figure 2).
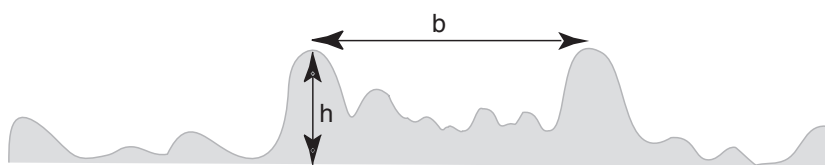
Figure 2. A schematic drawing of a roughness profile of a typical substrate. Here *h* is the average height of the hills and *L* the horizontal correlation length. The ratio of *h*/*L* can be interpreted as a crude measure of the roughness (see [43] for the exact definition). The drawing is not to scale.

3. Experimental procedure

In our measurements, we used two well-known techniques for determining the film thickness, namely surface plasmon spectroscopy (SPS) and ellipsometry. SPS has been applied for measuring film thicknesses on the surface of Au [23], while ellipsometry has been used for measurements on the surface of Si [28]. The substrate was mounted vertically inside a copper cell. The adsorbate was condensed into the cell through two small capillaries which were fed into the cell from the top. The capillaries, which also served as evacuation lines of the cell, were then blocked after completion of the adsorption. The optical access to the surface was through optical windows symmetrically placed in a fourfold geometry. The experimental cell was mounted into a ^{4}He cryostat.
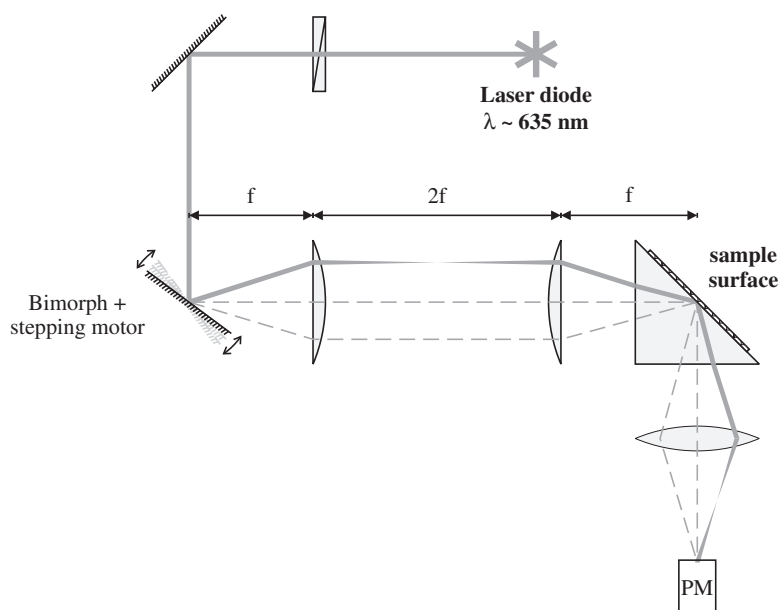
3.1. Surface plasmon spectroscopy

Surface plasmon spectroscopy is done by using P-polarized laser light on Au substrates. The light beam is resonantly coupled into surface plasmons at a certain incidence angle [44, 45] and focused on a photodiode placed outside of the cryostat. When a hydrogen film is adsorbed this causes a resonance detuning. Measuring the shift of the resonance angle allows us to determine the average thickness of the film adsorbed on the surface. Figure 3 illustrates schematically the SPS set-up. Using this method, thicknesses of less than a monolayer up to a few hundred nanometres can be resolved.
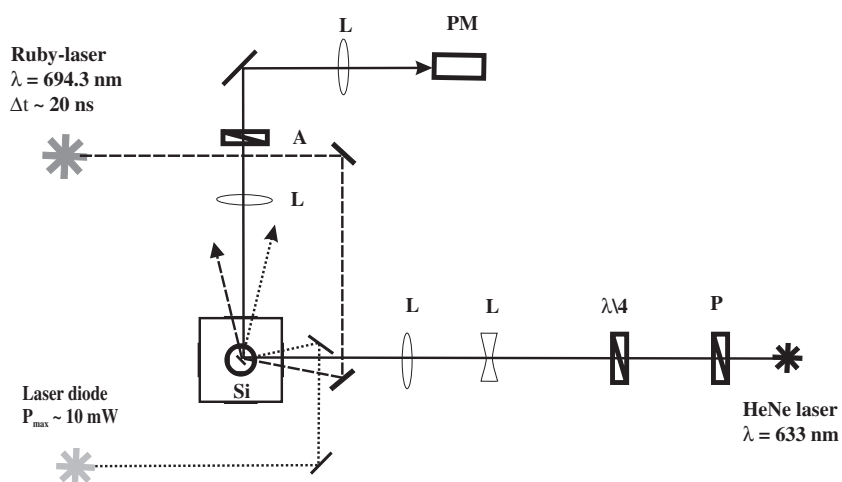
3.2. Ellipsometry and laser annealing

For measurements on Si, a standard null-ellipsometry set-up was built up. This worked on the basis of the minimization of the reflected intensity upon reflection from the surface [46].

In figure 4 a schematic drawing of the ellipsometry set-up is shown. The ellipsometer is in a usual PCSA configuration, where P, C, S, and A stand for polarizer, quarter-wave plate, sample, and analyser (see also the figure caption). In a conventional null ellipsometer, the minimum (null) intensity, detected by a photodetector, can be obtained by properly setting A and P. Then, during adsorption the continuous rotational adjustment of A and P allows one to stay always at the minimum. By using this configuration one can extract the angles Ψ and Δ from the rotation A and P angle values [47], from which the thickness of the films can be determined. We adopt the two linear approximation relations from Archer [48] for calculating the coverage. We note that this approximation holds as long as the film thicknesses do not exceed 100 Å. In experiments presented here, the overall thickness is always well below this value.

In addition to the ellipsometer set-up, another cw laser was used with which the local desorption–adsorption of the film could be manipulated (see figure 4). The reasons for this are discussed in section 4. Since studying the effect of surface roughness on the wetting behaviour

Figure 3. The main optical components of the surface plasmon spectroscopy set-up. The Au substrate, evaporated on the base of the prism, is placed inside an optical cryostat, cooled with ^{4}He.

Figure 4. The set-up for the ellipsometry and the laser annealing. The main components of the ellipsometer are drawn with a stronger contrast. The system works in a PCSA configuration, where P, C, S, and A stand for polarizer, quarter-wave plate ($\lambda/4$), substrate (Si), and analyser. The symbols PD, PM, and L are for the photodiode, the photomultiplier, and the lens. See the text for detailed explanations of the function of each component.

of adsorbates has been the goal of this work, *in situ* cleaning and annealing of Si have also been done and the details are discussed in section 4.2.4. The annealing set-up is shown in figure 4, together with the ellipsometry set-up (see [49, 50] for detailed information on laser annealing).
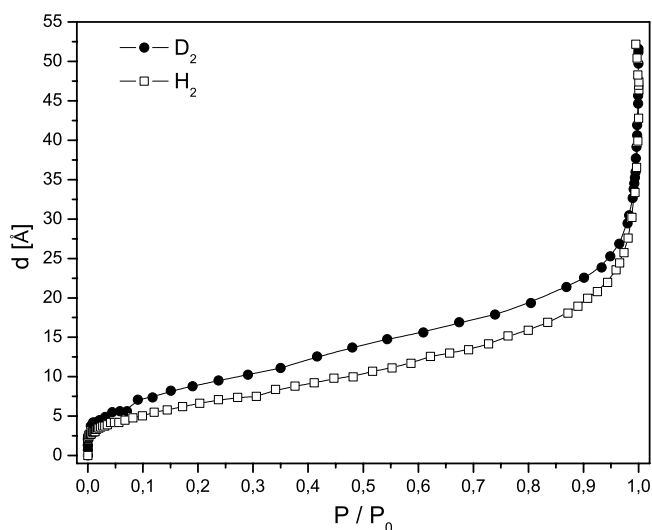
Figure 5. Adsorption isotherms of H_2 and D_2 at temperatures above the T_3 of H_2 and D_2. The thickness diverges as the saturated vapour pressure, P_0, is approached.

4. Results and discussion

In all the experimental runs presented here, first an adsorption isotherm was taken at a temperature well above the triple temperature of the respective adsorbate, as in earlier experiments [21–23, 28]. A sufficient amount of gas was condensed into the system that gas–liquid coexistence was reached, and bulk liquid formed at the bottom of the sample cell. (We should note that the films investigated were not exactly at coexistence, because the position of the optical measurement was located a few mm above the bulk surface, and furthermore the temperature of the film was slightly higher than the cell temperature due to unavoidable heating by the probe laser beam. This effect is not relevant, however, for relatively thin films below about 50 Å, which are the focus of this paper.) After taking the adsorption isotherm the cell was slowly cooled to temperatures well below T_3, with the amount of material in the cell being kept fixed, so the adsorbed film always had a thickness close to the equilibrium value at coexistence.

4.1. Adsorption isotherms above T_3

The results presented in this section are for the adsorption of H_2 and D_2 on the surface of a 45 nm thick Au layer evaporated onto a glass substrate (see figure 3). The data were taken using the SPS technique. Figure 5 shows the film thickness plotted as a function of the reduced pressure P/P_0, where P_0 is the saturated vapour pressure at the corresponding temperature. As the pressure is increased, the thickness first grows rapidly, then reaches an intermediate region of moderate growth, until eventually, close to P_0, it starts to diverge. This behaviour is qualitatively accounted for by the Frenkel–Halsey–Hill (FHH) theory [51–53], which predicts a logarithmic relationship between the film thickness d and the ambient pressure, given by $\alpha d^{-3} = k_B T \ln(P_0/P)$. Here, α and k_B are the Hamaker and Boltzmann constants, respectively. As shown by Vorberg *et al* [54], deviations in the adsorption isotherm from the FHH prediction which are observed in the intermediate region can be explained by a contribution of thermally excited capillary waves [55]. The slight difference in the film
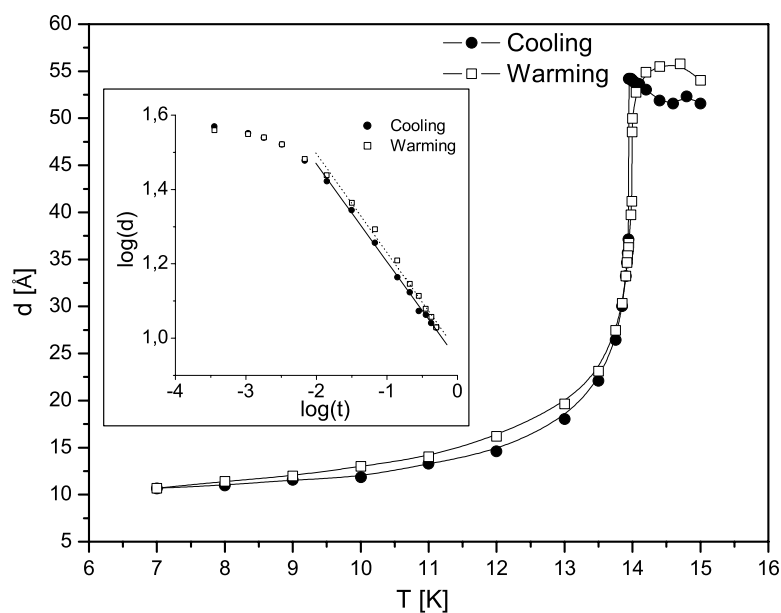
Figure 6. The temperature dependence of the film thickness of H_2 adsorbed on Au. In the inset, the same data are plotted on a logarithmic scale. Here t is the reduced temperature, defined as $t = (T_3 - T)/T_3$.

thickness of H_2 and D_2 in the intermediate region of figure 5 might also be due to thermal excitations, but more quantitative studies are necessary to draw final conclusions.

4.2. Wetting behaviour below T_3

4.2.1. H_2 and D_2 on Au.   The main goal of this work was to investigate the adsorbed films close to coexistence in the temperature range below T_3, where the bulk material is solid. Typical heating/cooling cycles for H_2 and D_2 on a gold substrate are shown in figures 6 and 7, respectively. The rate of the temperature change was controlled as typically 20 mK min^{-1}, which ensured conditions close to thermodynamic equilibrium. The behaviours observed for the two adsorbate materials are quite similar: whereas above T_3 the adsorbed film is rather thick with an essentially constant value of d, the thickness drops steeply upon cooling below T_3, and at low T eventually levels off at a value around 10 Å, corresponding to about three molecular monolayers. Only a slight hysteresis between cooling and warming is seen, which confirms that the data were taken close to equilibrium. This triple-point wetting behaviour has been observed to be universal for almost all van der Waals adsorbates, in particular the noble gases [11–13]. It can be explained by assuming that only a few layers of the film are solid (which determine the thickness at $T \ll T_3$). The increase in thickness close to the triple point is ascribed to a liquid layer on top of the solid, which grows quickly as the liquid–gas coexistence vapour pressure is approached at T_3. On this basis, one expects the temperature dependence of the film thickness close to T_3 to follow a relation $d(T) \propto [(T_3 - T)/T_3]^{-\beta}$, with $\beta = 1/3$ [20]. The insets in figures 6 and 7, where the data are plotted on a logarithmic scale, show that the data do indeed follow a power law over a considerable temperature range, and that the exponent is in reasonable agreement with the prediction: in the case of D_2 the fit yields $\beta = -0.30 \pm 0.003$ and 0.29 ± 0.003 for warming and cooling, respectively, and in the case of H_2 the corresponding values are $\beta = -0.26 \pm 0.005$ and -0.27 ± 0.008.
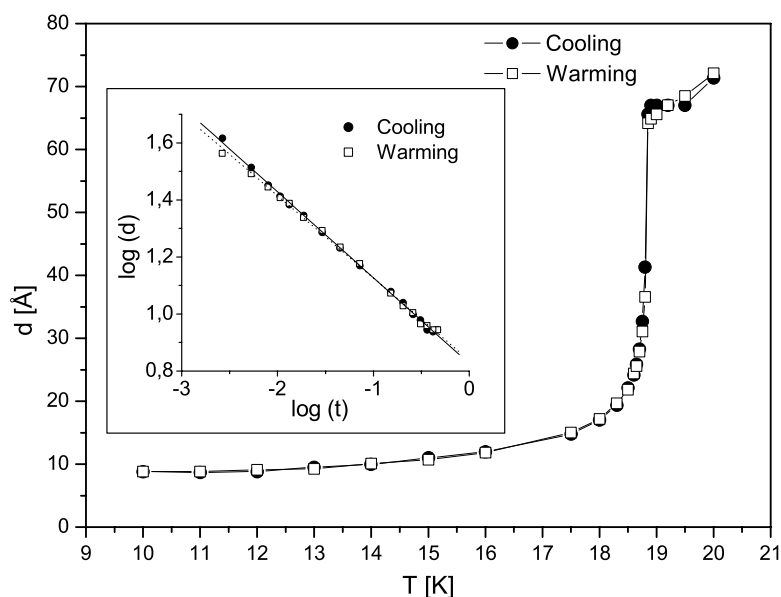
Figure 7. Wetting curves of D_2 on Au are shown. A similar behaviour has been observed for other kinds of adsorbates. In the inset, the same curves are plotted on a logarithmic scale.

At this point the comparison between the measured solid thickness at $T \ll T_3$ and the prediction of theory appears adequate: for H_2 on Au the value of the reduced substrate strength is $R = 4.5$ [43]. As seen from figure 1, for this value of R the solid film should be thicker than 100 Å, corresponding to 30 monolayers, if we assume a smooth substrate as in the GS theory [5]. From the fact that experimentally only a solid layer of about three monolayers is observed, we conclude that the substrate roughness plays an essential role here [43] (see the dotted curve in figure 1). Thus evaporated gold films, although optically smooth, appear rough on the atomic scale which is relevant for the wetting behaviour. This aspect is further investigated below for Si substrates, which are considerably smoother than our gold films (see section 4.2.3).

4.2.2. Preplating and mixtures. 'Preplating' means depositing a few monolayers of another adsorbate in advance, before the adsorption of the main adsorbate under investigation. By doing this, the interaction between the substrate and the adsorbate can be tailored, and by choosing a proper preplating material an effective substrate strength R_{eff} which is smaller than the R without preplating may be achieved. This could lead to wetting of the solid, and is indeed another aspect of the GS theory, which predicts a different solid thickness depending on the kind of preplating adsorbate [5].

For H_2 on Au, preplatings with Ar, Ne, and CH_4 have been done already, some time ago [21]. Similar experiments followed for D_2 on Al and graphite (HOPG) with Ar, Ne, CH_4, and C_2H_6 [26]. Although in some cases a slight increase of the solid thickness was achieved, the overall effect of dewetting by the solid film continued to exist [21]. We have also studied the effect of Ar and CH_4 preplated Au on the H_2 wetting. Our results agree with previous experiments. In addition, we used D_2 as a preplating material, and investigated the H_2–D_2 mixed systems. This was done by taking adsorption isotherms of D_2 above its T_3. Then, the temperature was lowered and stabilized at some temperature near, but still well above,
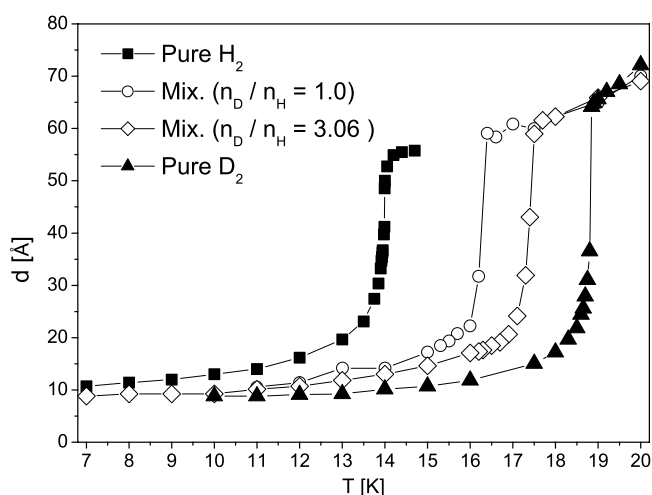
Figure 8. Wetting curves of pure and mixed systems of H_2 and D_2. The data demonstrate the existence of an effective triple point, $T_3^{(eff)}$, which depends on the species concentration of the H_2–D_2 mixture. The value of $T_3^{(eff)}$ always falls between $T_3^{(H_2)}$ and $T_3^{(D_2)}$.

the T_3 of H_2. At this point a thin solid layer of D_2 has formed on the surface of Au. The adsorption of H_2 on top of the existing D_2 film until saturation was reached followed before temperature scans below the T_3 of H_2 were carried out. The temperature was then increased and stabilized at about 30 K, a temperature far above T_3 of D_2. A H_2–D_2 mixture with certain species concentration was prepared and the whole system was kept at this temperature for hours. This was done to obtain a homogeneous mixture. The speed at which the temperature was changed was again about 20 mK min^{-1}.

The results of these experiments are presented in figure 8 (see [22, 23] for detailed discussions). It was found that an effective triple point $T_3^{(eff)}$ can be defined for a mixed system which falls always between the T_3 of H_2 and D_2, depending on the concentration of the species. Additionally, no significant change in the thickness of the solid layer is observed.

As a consequence of these preplating and mixture experiments we conclude that the dewetting below T_3 is a rather robust phenomenon which for the substrates discussed so far hardly depends on subtleties such as details of the interaction strength. This suggests that a more general aspect dominates here. We show in the next section that the key to the problem appears to be the substrate roughness, as already indicated above.

4.2.3. Wetting on Si. We now discuss the results for the wetting of Si substrates, which are very smooth and can, in addition, conveniently be cleaned by laser annealing. The typical rms roughness of an Au substrate is measured to be about 1.3 nm; for commercial Si wafer surfaces it is ∼0.15 nm [28], one order of magnitude smoother. The van der Waals interactions for H_2 on Au and Si are nearly the same [40, 56–58]. Using the calculations of Vidali and Cole [56] we get 8739 and 6276 K Å^3 for H_2/Au and H_2/Si, respectively, with estimated uncertainties of about 20% arising from the applied approximations. Considering the fact that the film thickness is proportional to the cubic root of the vdW coefficient, Si and Au should essentially behave similarly with respect to substrate strength. It is therefore likely that—should differences in the wetting behaviour of our Au and Si surfaces be observed—they can be ascribed to the different surface topography.
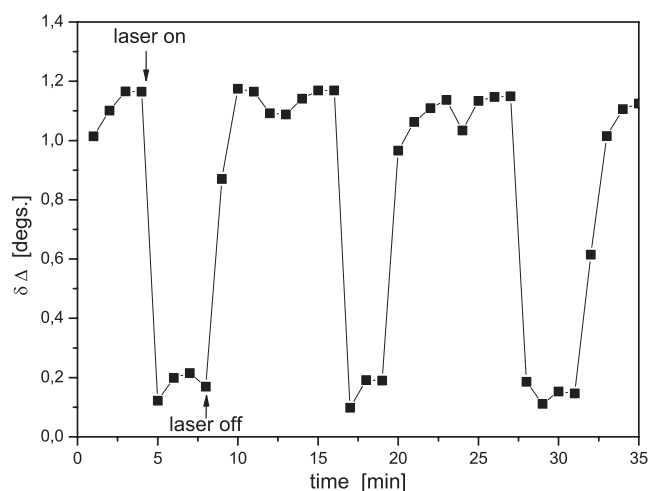
Figure 9. A real time snapshot of the change of the ellipsometer angle $\delta\Delta$ (and hence the film thickness) of a saturated liquid H_2 film on Si upon laser heating is shown. The temperature is about 14 K, slightly above T_3 for H_2. The thickness decreases (as $\delta\Delta$ decreases) as the heating laser is switched on, and comes back to the original value before heating when the heating laser is turned off.

The measurements on Si were done by means of ellipsometry as described in section 3.2. The ellipsometer is very sensitive to polarization effects, such as strain-induced birefringence in the quartz windows, and, as a result, the position of the minimum may shift upon temperature ramping. In order to reduce such effects due to drift, we applied in this case a differential method: in addition to the ellipsometer probe laser (power 100 μW) a heating laser (10 mW) was focused onto the probe spot, which was periodically switched on and off at a frequency of 3 mHz (see figure 9). In the 'on' state the intensity of the heating laser was sufficient to desorb the major part of the adsorbed film (apart from three monolayers which appeared to be more strongly bound). In the 'off' state the film quickly recovered to its initial thickness without a heating laser, as shown in figure 9. The difference between 'on' and 'off' thus provides information about the film thickness (apart from the remaining strongly bound layer) free of drift effects. The data in figures 10–12 were obtained with this method.

Figure 10 shows results for H_2 on Si determined in this way. The thickness saturates below 13 K at a value of 0.32 in units normalized to the thickness above T_3 (which is 55 ± 5 Å), corresponding to 17.5 Å. Compared to the value on rough Au ($d \approx 10$ Å) the thickness is thus significantly increased. This effect is also illustrated in figure 11, which shows the film thickness on Si on a logarithmic scale, like in the inset of figure 6. Again a power law is observed with a value of $\beta = 0.31 \pm 0.02$ in this case, but in contrast to the case for figure 6 the data display a clear deviation from this law for $\log(t) > -1.60$, where the thickness starts to saturate. We interpret this saturation at low temperatures as evidence for the solid H_2 forming a distinctly thicker film on the smooth Si substrate.

Similar measurements were done for D_2 on Si, and the data, shown in figure 12, corroborate the results for H_2.

4.2.4. Laser cleaning and annealing. Here we discuss our first results obtained from measurements on *in situ* cleaned and annealed Si substrates. The idea of the laser cleaning is to remove unwanted contaminations (e.g. water) from the Si surface, which adsorb while mounting the substrate into the cell at room temperature and ambient atmosphere or during
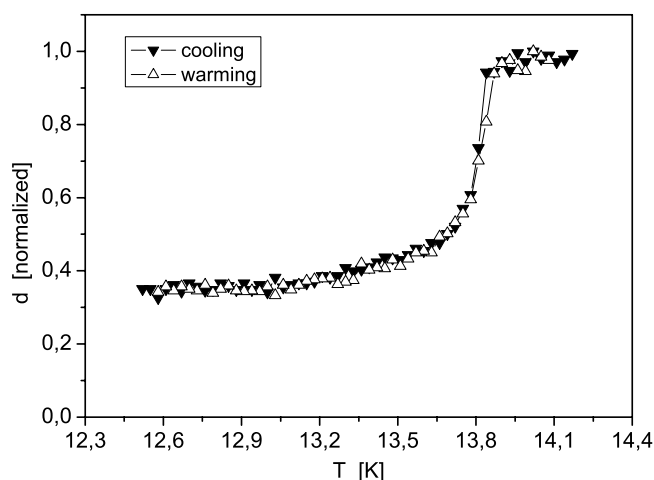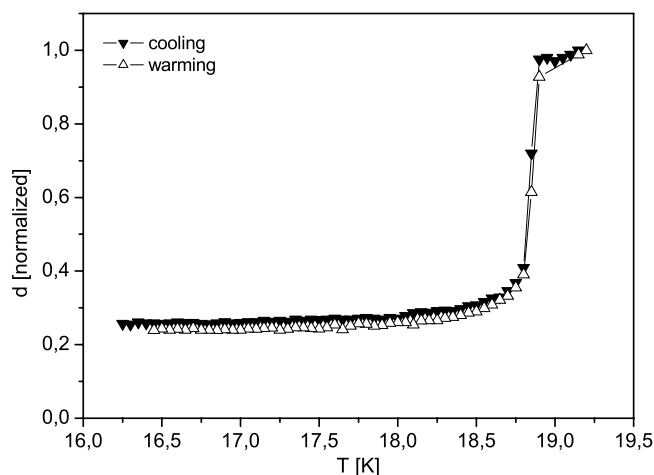
Figure 10. Shown is the wetting behaviour of H_2 on Si. d is normalized to the thickness in saturation above T_3 of H_2.
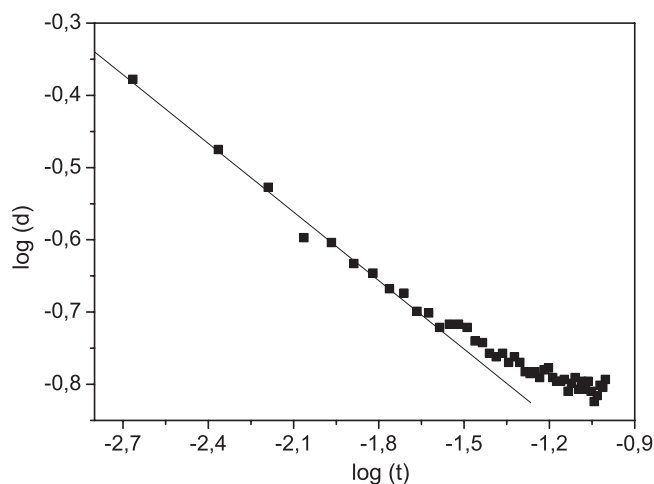
Figure 11. Illustrated is the warming curve of figure 10 plotted on a logarithmic scale. The slope of the straight line is 0.31.

cooling down the cell (we do not have UHV conditions). For the cleaning procedure, we focus the light of a powerful laser diode (200 mW) on the same area of the substrate where the ellipsometry beam hits the surface. This is done at the beginning of the experiment, and the laser light is continuously left on while cooling the cell from room temperature down to the working temperature. In this way we can keep the temperature of the substrate about 30 K above the ambient temperature in the cell. The colder cell walls thus act as a trap for any desorbed material from the Si substrate, and moreover prevent contamination of the sample surface during cooling down. We found from other experiments that most of the usual contaminations of a cooled substrate surface can be considerably reduced by this procedure [59].

After reaching low temperature (14.2 K), the cell was kept for several hours under these conditions. Then the cleaning laser was switched off, and after establishing thermal equilibrium

Figure 12. Depicted is the wetting behaviour of D_2 on Si. The thickness is normalized to the one in saturation above T_3.

between cell and substrate, an adsorption isotherm of H_2 was performed. In the next step the cell was slowly cooled and warmed between 9 and 14.2 K. The observed T_3 wetting behaviour and solid H_2 film thickness determined, however, were about the same as measured for uncleaned Si substrates (figure 10). This shows that standard contaminations of the Si surface have no crucial influence on the wetting behaviour.

In the next step, after the second cooling, the temperature was fixed at 9 K, and the laser annealing procedure, using the ruby laser set-up shown in figure 4, was performed. Upon annealing the Si substrate, the H_2 film thickness increased by about two monolayers. Then we varied the temperature between 3.5 and 14 K. The overall thickness in this temperature range, where only the solid film is present, remained indeed somewhat larger. Yet the typical T_3 wetting behaviour was observed, i.e., incomplete wetting of the solid hydrogen film. At the end of the experiment the surface quality of the Si was analysed by SEM. No sign of laser-induced damage were seen on the area where the measurements were done.

Although we observed only a small increase in the thickness of the solid film this result is promising and in qualitative agreement with the calculations of Esztermann *et al* [43]. Clearly more experiments are needed to check the influence of surface roughness on the growth of a solid hydrogen film and to compare more quantitatively with the theory. For that it is not only necessary to manipulate the surface of the substrate, but also to characterize this surface on the atomic scale. Therefore we have built a new set-up which allows both measurements of the film thickness, manipulation of the surface of the substrate, and *in situ* characterization via a low temperature scanning tunnelling microscope [59].

5. Summary and conclusions

An early theory [5] predicts that the induced strain from the substrate underneath an adsorbed solid film, e.g. due to lattice mismatch between substrate and film, is responsible for incomplete wetting of this film. This effect of dewetting can be amplified by the roughness of the substrate, as predicted by a recent theory [43]. Motivated by these ideas we investigated the effect of T_3 wetting of molecular H_2 isotopes and checked the influence of the roughness of the substrate. For that we used different substrates, namely thermally evaporated gold films on glass and on

bare Si wafers. The latter provide a much smoother surface. In addition we tried to manipulate the surface of the Si (by laser cleaning and annealing) *in situ* in order to vary the roughness properties. As a third parameter we tuned the interaction strength between adsorbate and substrate by preplating with different noble gases. We also used D_2 as preplating material and, in this context, investigated the mixing properties and the dewetting of the solid phase of this binary system (by the two hydrogen isotopes).

It turned out that for all variations that we have considered for the substrates the usual dewetting of the solid phase below T_3 was observed. However, small differences in the adsorbed solid film thickness could be detected. Comparing the hydrogen thickness on Au and Si showed at $T \ll T_3$ an increase from about three to five solid layers of hydrogen. Additional laser cleaning of the Si surface did not result in any difference; however, a further increase of about two layers of solid hydrogen was measured on an annealed Si surface. These changes were less than expected. Still, they are very promising for the goal of achieving complete wetting of solid hydrogen films, and they are, at least qualitatively, in agreement with the recent calculations [43]. Further investigations on modifying the substrate properties (i.e., decreasing the surface roughness) are on the way, together with simultaneous (i.e., *in situ*) characterization of the substrates used and modified on the necessary nanometre scale.

Acknowledgment

References

[1] Dash J G and Puff R D 1981 *Phys. Rev.* B **24** 295
[2] Pandit R, Schick M and Wortis M 1982 *Phys. Rev.* B **26** 5112
[3] Pandit R and Fisher M E 1983 *Phys. Rev. Lett.* **51** 1772
[4] Huse D A 1984 *Phys. Rev.* B **29** 6985
[5] Gittes T F and Schick M 1984 *Phys. Rev.* B **30** 209
[6] Dietrich S 1988 *Phase Transitions and Critical Phenomena* vol 12, ed C Domb and J L Lebowitz (London: Academic) p 1
[7] Schick M 1990 *Liquids at Interfaces* (*Les Houches Session XLVIII*) ed J Charvolin, J F Joanny and J Zinn-Justin (Amsterdam: Elsevier) p 415
[8] Youn H S and Hess G B 1990 *Phys. Rev. Lett.* **64** 443
[9] Youn H S, Meng X F and Hess G B 1993 *Phys. Rev.* B **48** 14556
[10] Hess G B 1991 *Phase Transitions in Surface Films* vol 2, ed H Taub, G Torzo, H J Lauter and S C Fain (New York: Plenum) p 357
[11] Migone A D, Dash J G, Schick M and Vilches O E 1986 *Phys. Rev.* B **34** 6322
[12] Rieutord F, Simon R, Conradt R and Buschbaum P M 1997 *Europhys. Lett.* **37** 565
[13] Mistura G, Ancilotto F, Bruschi L and Toigo F 1999 *Phys. Rev. Lett.* **82** 795
[14] Krim J, Dash J G and Suzanne J 1984 *Phys. Rev. Lett.* **52** 640
[15] Bruschi L and Mistura G 2000 *Phys. Rev.* B **61** 4941
[16] Daunt J G, Hedge S G, Tsui S P and Lerner E 1981 *J. Low Temp. Phys.* **44** 207
[17] Wu H and Hess G B 1998 *Phys. Rev.* B **57** 6720
[18] Migone A D, Hofmann A, Dash J G and Vilches O E 1988 *Phys. Rev.* B **37** 5440
[19] Leiderer P and Albrecht U 1992 *J. Low Temp. Phys.* **89** 229
[20] Albrecht U, Conradt R, Herminghaus S and Leiderer P 1996 *Low Temp. Phys.* **22** 117
[21] Klier J, Weichhard C and Leiderer P 2000 *Physica* B **284** 391
[22] Sohaili M, Klier J and Leiderer P 2001 *J. Low Temp. Phys.* **122** 249
[23] Tibus S, Sohaili M, Klier J and Leiderer P 2003 *Low Temp. Phys.* **29** 970
[24] Albrecht U, Evers P and Leiderer P 1993 *Surf. Sci.* **283** 419
[25] Albrecht U, Leiderer P and Kono K 1993 *Surf. Sci.* **283** 423

[26] Fleischmann L, Bonn J, Degen B, Przyrembel M, Otten E W, Weinheimr C and Leiderer P 2000 *J. Low Temp. Phys.* **119** 615
[27] Fleischmann L, Bonn J, Bornschein B, Leiderer P, Otten E W, Przyrembel M and Weinheimr C 2000 *Eur. Phys. J.* B **16** 521
[28] Angrik J, Sohaili M, Klier J and Leiderer P 2003 *Physica* B **329** 435
[29] Klistner T and Pohl R O 1986 *Phys. Rev.* B **34** 6045
[30] Kono K, Albrecht U and Leiderer P 1991 *J. Low Temp. Phys.* **83** 423
[31] Kono K, Albrecht U and Leiderer P 1991 *J. Low Temp. Phys.* **82** 279
[32] Monarkha Y P, Albrecht U, Kono K and Leiderer P 1993 *Phys. Rev.* B **47** 13812
[33] Otten O W 1994 *Prog. Part. Nucl. Phys.* **32** 153
[34] Backe H, Barth H, Balzhauser M, Bonn J, Degen B, Fleischmann L, Leiderer P, Moore R J, Otten E W, Schneller S, Przyrembel M and Weinheimer C 1994 *Prog. Part. Nucl. Phys.* **32** 173
[35] Otten O W 1995 *Prog. Part. Nucl. Phys.* **38** 26
[36] Davenport P H 1983 *Prospects for Fusion* ed W Marshal (Oxford: Clarendon)
[37] Craxton R S, McGroy R L and Sourer J M 1986 *Sci. Am.* **255** 60
[38] Wagner M and Ceperley D M 1994 *J. Low Temp. Phys.* **94** 161
[39] Wagner M and Ceperley D M 1996 *J. Low Temp. Phys.* **102** 275
[40] Vidali G, Ihm G, Kim H Y and Cole M W 1991 *Surf. Sci. Rep.* **12** 135
[41] Aziz R A 1984 *Inert Gases* ed M L Klein (Berlin: Springer) p 5
[42] Cheng E, Cole M C, Saam W F and Treiner J 1993 *Phys. Rev.* B **48** 18214
[43] Esztermann A, Heni M, Löwen H, Klier J, Sohaili M and Leiderer P 2002 *Phys. Rev. Lett.* **88** 55702
[44] Raether H 1986 *Surface Plasmons* (Berlin: Springer)
[45] Herminghaus S and Leiderer P 1989 *Appl. Phys. Lett.* **54** 99
[46] Azzam R M A and Bashara N M 1987 *Ellipsometry and Polarized Light* (Amsterdam: North-Holland)
[47] McCrakin F L, Passaglia E, Stromberg R R and Steinberg H L 1963 *J. Res. Natl Bur. Stand.* A **67** 363
[48] Archer R J 1963 *Ellipsometry in the Measurement of Surface and Thin Films* ed E Passaglia, R R Stromberg and J Kruger (Washington, DC: Symposium Proceedings) p 255
[49] Jellison G E, Lowndes D H, Mashburn D N and Wood R F 1986 *Phys. Rev.* B **34** 2407
[50] Boneberg J 1993 Dynamische verfestigung von halbleiterschichten nach ns-laser-annealing *PhD Thesis* University of Konstanz, Konstanz
[51] Halsey G D 1948 *J. Chem. Phys.* **16** 931
[52] Frenkel J 1949 *Kinetic Theory of Liquids* (London: Oxford University Press)
[53] Hill T L 1949 *J. Chem. Phys.* **17** 520
[54] Vorberg J, Herminghaus S and Mecke K 2001 *Phys. Rev. Lett.* **87** 196105
[55] Mecke K R and Krim J 1996 *Phys. Rev.* B **53** 2073
[56] Vidali G and Cole M W 1981 *Surf. Sci.* **110** 10
[57] Rauber S, Klein J R, Cole M W and Bruch L W 1982 *Surf. Sci.* **123** 173
[58] Schwartz C and Roy R J L 1986 *Surf. Sci. Lett.* **166** 141
[59] Zech M, Fubel A, Leiderer P and Klier J 2004 *J. Low Temp. Phys.* **137** 179